Electrical Conductivity Evaluation from Measurements in Strongly Coupled Tungsten and Aluminum Plasmas[1]

K.V. Khishchenko, P.R. Levashov, S.I. Tkachenko

Institute for High Energy Densities, Joint Institute for High Temperatures, Russian Academy of Sciences, Izhorskaya 13/19, Moscow, 125412, Russia, Phone: +74954842456, Fax: +74954857990, E-mail: konst@ihed.ras.ru

Abstract – We study the influence of equation-of-state (EOS) model on the evaluation of electrical conductivity from measurements in strongly coupled plasmas of tungsten [4] and aluminum [5]. Three different semiempirical EOS models for metals are used. Multi-phase EOS model takes into account the melting, evaporation, and ionization effects; this EOS adequately describes the set of experimental data available for tungsten and aluminum at high pressures and temperatures. Caloric EOS model disregards phase transitions; however it describes shock-wave data within a good accuracy. The soft-sphere EOS model allows for evaporation of metals and has been calibrated using isobaric expansion experiments but does not take into account melting and gives understated density at normal temperature and pressure. Discrepancies in obtained thermodynamic parameters and resistivity values as compared with simulation results from [4, 5] are analyzed.

1. Introduction

Strongly coupled plasma is commonly used in fundamental research and applications [1]. Electrical explosion is an effective way to study thermodynamic and transport properties of metals in both condensed and plasma states at high energy densities [2, 3].

Measurement of the heating current and voltage as functions of time allows one to calculate the electrical resistance of wire or foil under study. To determine the electrical resistivity of a metal the cross-section area of the conductor during the process of expansion should be known also. If geometric sizes of the sample have not been measured simultaneously with current and voltage it is reasonable to use the results of numerical simulation. In this case calculated characteristics of matter are determined, in particular, by an equation-of-state (EOS) model.

In the present work we study the EOS model influence on the electrical conductivity values of strongly coupled plasmas based on experimental data for tungsten [4] and aluminum [5].

2. Description of experiment

The experiments on electrical conductivity measurement with tungsten [4] and aluminum [5] were carried out in a plane geometry. A metal foil stripe with the length $l_z = 10$ mm, width $h = 1.5$ mm, and thickness $2a = 20$ μm was placed between two glass or sapphire plates with the thickness $a_1 = 5$ mm. Side slits were shielded with thin mica stripes. In the experiments under consideration the skin layer thickness δ is significantly larger than the foil thickness.

Cartesian coordinate system is introduced as follows: x-axis is perpendicular to the foil plate, y-axis is directed along the smaller side of the foil, and z-axis — along the bigger side. In 1D process the foil expands along the x-axis, the magnetic induction B is directed along the y-axis, and the heating current I as well as the electric field intensity E are directed along the z-axis.

The foil was heated by the power current pulse; the time dependencies of the current through the sample $I(t)$ and voltage drop $U(t)$ were registered. Then it was calculated the resistive part of the voltage drop $U_R(t)$, electrical resistance $R(t) = U_R(t)\, I^{-1}(t)$ and Joule heating rate $Q_t(t) = U_R(t)\, I(t)$. Other values required for conductivity calculation can be obtained by means of numerical simulation. Assuming that the current density j is distributed uniformly over the cross-section of the foil and depends only on time, i.e. $j(t) = I(t)\, S^{-1}(t)$, where $S(t) = 2a(t)\, h$, from the Maxwell equation $j(t) = \mu^{-1} \partial B/\partial x$ (SI system of units is used, μ is the magnetic permeability) one can calculate $B(t, x) = \mu\, I(t)\, x\, S^{-1}(t)$. So it is possible to determine foil parameters as functions of t and x numerically solving only a set of hydrodynamic equations with the Ampere force $jB = \mu\, I^2(t)\, x\, S^{-2}(t)$ and energy input $jE = Q_t(t)\, V^{-1}(t)$, where $V(t) = S(t)\, l_z$ is the foil volume.

The results of calculation by such a technique not allowing for magnetic field diffusion were presented in [4, 5].

[1] The work was supported by the Grants of the Russian Foundation for Basic Research No. 04-02-17292, 05-02-16845, and 05-02-17533.

3. EOS models

The EOS model for tungsten and aluminum used in [4, 5] to interpret the measurements results is based on the soft-sphere EOS [6] and takes into account ionization effects according to the mean ion model [7]. This EOS is unpublished and this fact prevents us from evaluating its quality in comparison with available experimental data at high temperatures and pressures.

We used three different semiempirical EOS models for metals [6, 8–10].

Multi-phase EOS [8, 9] in a form of functions $P = P(\rho, T)$ and $\varepsilon = \varepsilon(\rho, T)$ (EOS1), where P is the pressure, T is the temperature, ρ is the density, ε is the specific internal energy, takes into account the effects of melting, evaporation, and ionization. This EOS adequately describes the set of experimental data on isothermal and shock compression as well as on adiabatic and isobaric expansion of metals, see details for tungsten in [8] and for aluminum in [9].

Caloric EOS [10] in a functional form $P = P(\rho, \varepsilon)$ (EOS2) disregards phase transitions; however it describes shock-wave data for condensed and rarefied states within a good accuracy.

The soft-sphere EOS [6] as functions $P = P(\rho, T)$ and $\varepsilon = \varepsilon(\rho, T)$ with coefficients from [11] for tungsten and [12] for aluminum (EOS3) allows for evaporation of metal and has been calibrated using isobaric expansion experiments but does not take into account melting and gives understated density at normal temperature and pressure. Imitating the approach [11] in the present work for EOS3 model of aluminum we used higher value of heat capacity at $T \to \infty$ than in [12] to correctly reproduce experimental value of the liquid phase enthalpy at melting temperature and atmospheric pressure.

To describe the properties of glass and sapphire we used caloric EOS $P = P(\rho, \varepsilon)$ [13].

4. MHD modeling

Assuming that spatial perturbations of the sample form are small and electron and ion temperatures are the same, as well as neglecting the thermal conductivity effect, the set of 1D magnetohydrodynamic (MHD) equations in Lagrangian description for the foil heating can be written as follows:

$$\mathrm{d}m/\mathrm{d}t = 0\,, \tag{1}$$

$$\rho\,\mathrm{d}v/\mathrm{d}t = -\partial P/\partial x - (2\mu)^{-1}\,\partial B^2/\partial x\,, \tag{2}$$

$$\rho\,\mathrm{d}\varepsilon/\mathrm{d}t = -P\,\partial v/\partial x + j^2/\sigma_w\,, \tag{3}$$

$$\mathrm{d}(\mu B)/\mathrm{d}t = \partial\left[\sigma_w^{-1}\,\partial B/\partial x\right]/\partial x\,, \tag{4}$$

where m is the mass, v is the particle velocity, σ_w is the electrical conductivity.

The initial conditions for the set of equations (1)–(4) are written as follows: $\rho(x, 0) = \rho_0$, $v(x, 0) = 0$, $P(x, 0) = P_0$, $B(x, 0) = 0$.

The conditions on the symmetry plane $x = 0$ and on the surface $x = a(t)$ of the foil, as well as on the outer boundary of the glass or sapphire plate $x = a_1$ are as follows: $v(0, t) = 0$, $v(a, t) = \mathrm{d}a/\mathrm{d}t$, $v(a_1, t) = 0$, $\partial P/\partial x\,|_{x=0} = 0$, $P(a - 0, t) = P(a + 0, t)$, $P(a_1, t) = P_0$, $B(0, t) = 0$, $B(a, t) = \mu I(t)/2h$. Here ρ_0 and P_0 correspond to the normal conditions.

The conductivity was determined by the relation

$$\sigma_w(t) = I(t) l_z [U_R(t) S(t)]^{-1} \tag{5}$$

using the experimental dependencies $I(t)$ and $U_R(t)$ [4, 5] except for the stage of heating up to $T = T_1$, where $T_1 = 10$ kK for tungsten and 2.9 kK for aluminum.

In case of EOS1 at temperatures $T < T_1$ we used the semiempirical formulae [14–16] for the electrical conductivity $\sigma_w = \sigma_w(\rho, T)$ allowing for melting instead of experimental functions because of noise on the measured time dependence of voltage at the initial stage. According to [14] the electrical conductivity of the solid and liquid phases is determined by

$$\sigma_i = \sigma_{0i}\,\frac{(\rho/\rho_{0i})^{\delta_i}}{1 + \beta_i (T - T_{0i})}\,, \tag{6}$$

where $i = s$ corresponds to the solid, $i = l$ — to the liquid phase; $\rho_{0s} = \rho_0$; $T_{0s} = T_0$; ρ_{0l} and T_{0l} equal to the density of liquid phase and temperature at melting point under atmospheric pressure; σ_{0i}, β_i, and δ_i are chosen from analysis of experimental data [3, 14, 17]. The electrical conductivity of the two-phase state in the melting region is defined [15, 16] as

$$\sigma_{s+l} = \nu\sigma_s + (1 - \nu)\sigma_l\,, \tag{7}$$

where ν is the mass concentration of the solid phase,

$$\nu(\rho, T) = \frac{\rho_m^{-1}(T) - \rho^{-1}}{\rho_m^{-1}(T) - \rho_s^{-1}(T)}\,, \tag{8}$$

ρ_s and ρ_m are the densities of the solid and liquid phases on the melting curve.

In cases of EOS2 and EOS3 during the initial stage of heating we used time dependence of voltage $U_R(t)$ obtained in numerical modeling with EOS1 to determine the electrical conductivity according to (5).

5. Results

We carried out a number of simulations of the experiment using 1D MHD model as described in the previous section.

The calculated pressure in the tungsten foil between two glass plates and aluminum foil between two sapphire plates depending on the specific internal energy and temperature is shown in Fig. 1–4 in comparison with calculated results from [4, 5].

It can be seen that the melting process leads to oscillations of pressure $P(\varepsilon)$ and $P(T)$ near the symmetry plane of the tungsten foil (see the curves for

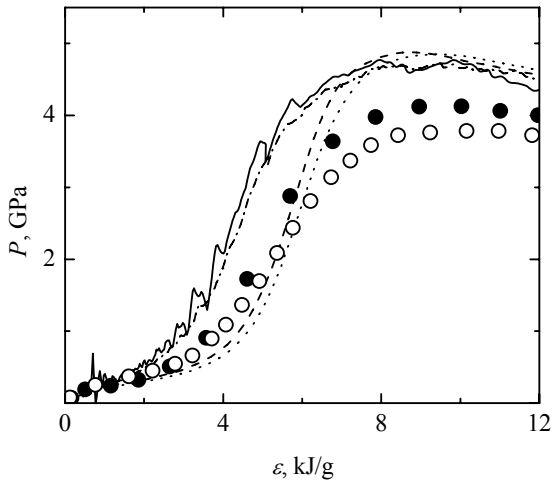

Fig. 1. Pressure versus specific internal energy in the tungsten foil during heating: open circles are from [4], lines and solid circles denote results of numerical simulation of present work in case of EOS1 (solid and dash-dotted lines, for layers $x = 0$ and $a(t)$ correspondingly), EOS2 (dashed and dotted lines, $x = 0$ and $a(t)$ correspondingly), and EOS3 (solid circles, $x = 0$)

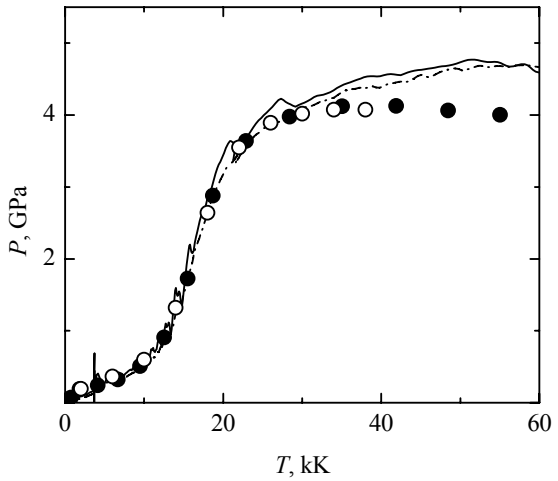

Fig. 2. Pressure versus temperature in the tungsten foil during heating: the notations are analogous to Fig. 1

EOS1 at $x = 0$ in Fig. 1–4). If melting is disregarded (like in calculations with EOS2 and EOS3 models) the pressure dependencies $P(\varepsilon)$ and $P(T)$ are smooth.

The dynamics of the process is to some extent determined by the EOS model. In case of tungsten the maximum relative difference between pressure values calculated with EOS1 and EOS2 is $\Delta P/P \sim 2$.

Fig. 1 and 2 show that the simulation with EOS3 gives the closest values of the pressure in the process of tungsten foil heating to that from [4]; this coincidence can be explained by similar EOS models used in these calculations. On the contrary, Fig. 4 shows that the calculated pressure for aluminum [5] maximally differs from the result of simulation with EOS3, $\Delta P/P \sim 1$.

One can see in Fig. 1 and 2 that parameters in the tungsten foil are distributed homogeneously except for the moment of melting which is clearly distinguishable by pressure oscillations. However, inhomogeneity in temperature distribution appears at the late stage of the expansion process.

In case of aluminum density and temperature are distributed almost uniform across the foil during the whole process of heating.

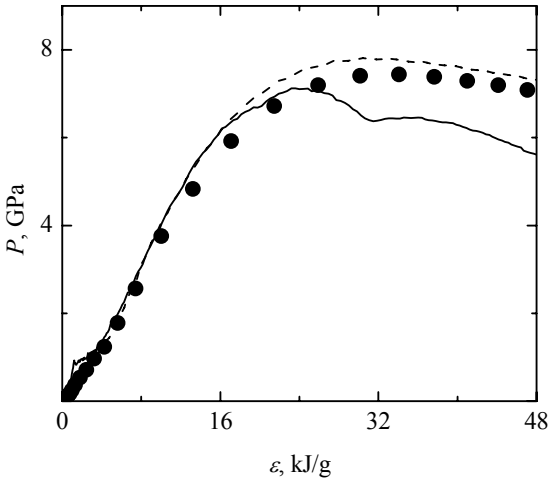

Fig. 3. Pressure versus specific internal energy in the aluminum foil during heating: the notations are analogous to Fig. 1

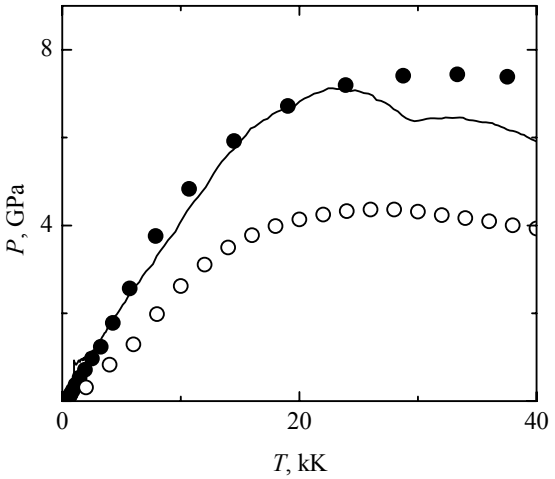

Fig. 4. Pressure versus temperature in the aluminum foil during heating: open circles are from [5], for the remaining notations, see the caption to Fig. 1

Distinctions in the methodology of simulation and description of thermodynamic properties of tungsten lead to systematically higher values of electrical resistivity $\rho_w = \sigma_w^{-1}$ in our interpretation than in [4], maximum relative difference is about $\Delta\rho_w/\rho_w \sim 0.6$ (Fig. 5).

In case of aluminum the maximum relative difference between values of electrical resistivity from [5] and from our evaluation is not less than $\Delta\rho_w/\rho_w \sim 1$ (Fig. 6).

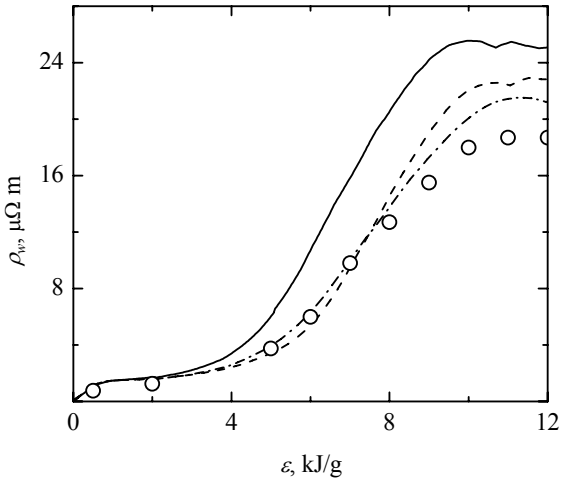

Fig. 5. Electrical resistivity of tungsten versus specific internal energy in the foil during heating: circles denote the results of simulations [4], lines correspond to presented modeling with EOS1 (solid line), EOS2 (dashed line), and EOS3 (dash-dotted line)

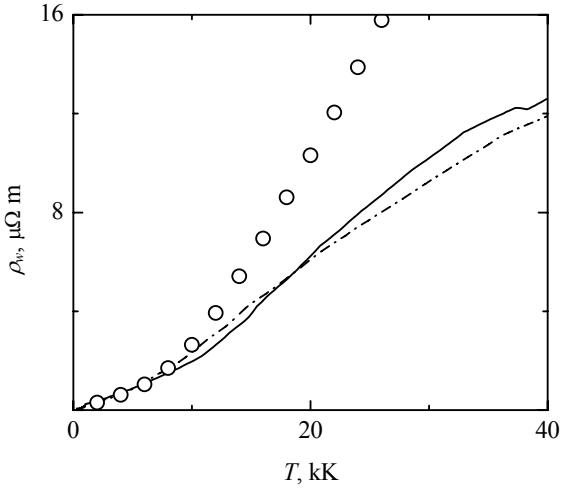

Fig. 6. Electrical resistivity of aluminum versus temperature in the foil during heating: circles denote the results of simulations [5], for the remaining notations, see the caption to Fig. 5.

6. Conclusion

In this work we have analyzed the results of electrical conductivity measurements in strongly coupled tungsten and aluminum plasmas using 1D MHD simulation and different EOS models.

The dynamics of the foil heating by the power current pulse is determined by the EOS model giving rise to distinctions in electrical resistivity values up to 60% for tungsten and more than 100% for aluminum.

These facts indicate that even in the case of the foil-heating regime [4, 5] with certain efforts to achieve homogeneous distribution of parameters for simplifying interpretation, there are still open problems to treat experimental data. We believe that further investigations of thermodynamic and transport properties of tungsten and aluminum plasmas will be helpful for the creation of adequate EOS as well as electrical conductivity models over a wide range of densities and temperatures.

The authors are grateful to V.N. Korobenko, A.D. Rakhel, and A.I. Savvatimski for valuable comments.

References

[1] V. Fortov, I. Iakubov, and A. Khrapak, *Physics of Strongly Coupled Plasma*, New York, Oxford University Press, 2006.
[2] S.V. Lebedev and A.I. Savvatimskii, Sov. Phys. Uspekhi **27**, 749 (1984).
[3] G.R. Gathers, Rep. Progr. Phys. **49**, 341 (1986).
[4] V.N. Korobenko, A.D. Rakhel, A.I. Savvatimskiy, and V.E. Fortov, Plasma Phys. Rep. **28**, 1008 (2002).
[5] V.N. Korobenko, A.D. Rakhel, A.I. Savvatimski, and V.E. Fortov, Phys. Rev. B **71**, 014208 (2005).
[6] D.A. Young, *A Soft-Sphere Model for Liquid Metals*, Lawrence Livermore Laboratory Report UCRL-52352, Livermore, 1977.
[7] M.M. Basko, High Temp. **23**, 388 (1985).
[8] K.V. Khishchenko, in *Physics of Extreme States of Matter — 2005*, ed. by V.E. Fortov et al., Chernogolovka, IPCP RAS, 2005, pp.170-172.
[9] K.V. Khishchenko and V.E. Fortov, in *Physics of Extreme States of Matter — 2002*, ed. by V.E. Fortov et al., Chernogolovka, IPCP RAS, 2002, pp.68-70.
[10] K.V. Khishchenko, Tech. Phys. Lett. **30**, 829 (2004).
[11] H. Hess, A. Kloss, A. Rakhel, and H. Schneidenbach, Int. J. Thermophys. **20**, 1279 (1999).
[12] P.R. Levashov, *Equations of State for Liquid Metals as a Soft-Sphere System*, Preprint JIHT RAS No. 1-446, Moscow, 2000.
[13] K.V. Khishchenko, I.V. Lomonosov, and V.E. Fortov, in *Shock Compression of Condensed Matter — 1995*, ed. by S.C. Schmidt and W.C. Tao, Woodbury, New York, AIP Press, 1996, pp.125-128.
[14] H. Knoepfel, *Pulsed High Magnetic Fields*, Amsterdam, North Holland, 1970.
[15] S.I. Tkachenko, K.V. Khishchenko, V.S. Vorob'ev, P.R. Levashov, I.V. Lomonosov, and V.E. Fortov, High Temp. **39**, 728 (2001).
[16] S.I. Tkachenko, K.V. Khishchenko, and P.R. Levashov, Int. J. Thermophys. **26**, 1167 (2005).
[17] N.I. Kuskova, S.I. Tkachenko, and S.V. Koval, J. Phys.: Condens. Matter **9**, 6175 (1997).